LOCAL COLLOCATION METHOD FOR SOLVING TIME DEPENDENT CONVECTION-DIFFUSION EQUATION

Jalil Rashidinia[1], Mahdie Mahdavi[1] , Amirhossein Sobhani[1]

[1]School of Mathematics, Iran University of Science and Technology, Narmak, Hengam, Tehran, Iran
e-mail: rashidinia@iust.ac.ir

Abstract. Local RBF collocation method based on multiquadric and inverse multiquadric basis has been presented for solving time-dependent convection-diffusion equation. Our purpose is to reduce the computational cost by providing matrix form of local collocation method. The approach is based on square stencils with sizes of 3×3 and 5×5 around each interior collocation point. This approach has been applied to solve two dimensional convection-diffusion equation by converting the problem to a sparse global system of linear equations with low condition number. The obtained numerical results verify the efficient and accurate nature of our method.

Keywords: Multiquadric and inverse multiquadric radial basis function, Time-dependent convection-diffusion equation, Finite collocation method.

AMS Subject Classification: 65M06, 65M70.

1. Introduction

Partial Differential Equations (PDEs) have been used to describe a wide variety of physical and engineering phenomena. Nowadays numerical solution of PDEs is one of the most common issues in applied mathematics (24,22). Many approaches have been developed to solve these equations, such as Finite Volume (FV), Finite Element (FE), Finite Difference (FD), spectral methods, Laplace transform, multiquadric trigonometric quasi-interpolation (18,14,21,1,31,10), but these approaches are limited to a mesh on domain and may not been effective in 5high-dimensional spaces. In real application, it is necessary to solve problems using of scattered data especially in multidimensional domains that it motivated scientists to investigate meshless methods (2, 5,6,11,13, 12, 17, 19). One of these meshless methods is Radial Basis Functions (RBFs). In 1990, for the first time, Edward Kansa (15,16) used RBF collocation method for solving partial differential equations.

Although RBF methods have high accuracy but are ill-condition. Many researchers bypassed this problem with various methods like preconditioning, domain decomposition (30,8) and use of compactly supported RBF that was proposed by Wendland and Wu (27,29).

An investigation for reducing of ill-conditioning is combining the Radial Basis Function and Finite Difference (RBF-FD) which is a local RBF collocation method

(3,7, 9,20, 23, 4, 28). In (26) the authors used finite collocation method for the steady state boundary value problem but in this paper we used their idea to develop a local collocation method for solution of following time dependent partial differential equation.

$$\frac{\partial u(x,t)}{\partial t} = L\left[u(x,t)\right] + \psi(x) \quad \text{in} \quad \Omega \tag{1}$$

$$u(x,0) = f(x) \qquad \text{in} \quad \Omega \tag{2}$$

$$B\left[u(x,t)\right] = g(x,t) \ , \quad \text{on} \quad \partial\Omega \tag{3}$$

where the operator L is defined by:

$$L = \left(k_x \frac{\partial^2}{\partial x^2} + k_y \frac{\partial^2}{\partial y^2} + v_x \frac{\partial}{\partial x} + v_y \frac{\partial}{\partial y} \right). \tag{4}$$

The outline of this manuscript as follow: In section 2, the discretization of time-dependent problems, by using finite difference method is given and local collocation method, finite collocation, on the square stencil is analyzed in this section. In section 3, the numerical results of proposed approach is presented that verify validity and accuracy of this approach and at the end, in section 4 conclusion is given.

2. Collocation method for time-dependent problems

In this section, by using temporal discretization of equations (1)-(3) based on finite difference method we have:

$$\frac{u^n - u^{n-1}}{\Delta t} = \theta L\left[u^n\right] + (1-\theta) L\left[u^{n-1}\right] + \Psi(x), \tag{5}$$

where $0 \le \theta \le 1$. Above equation can be written in following operator form

$$\bar{L}\left[u^n\right] = \hat{L}\left[u^{n-1}\right] + \Delta t \Psi(x), \tag{6}$$

where $\bar{L} = 1 - \theta \Delta t L$, $\hat{L} = 1 + (1-\theta)\Delta t L$.

Therefore at each time step a non-homogeneous boundary value problem is obtained. By denoting $\varphi(x) = \hat{L}\left[u^{n-1}\right] + \Delta t \Psi(x)$, the Eq.(6) can be reduced to a steady state problem. Hence we will have:

$$\bar{L}\left[u^n\right] = \varphi(x) \tag{7}$$

$$u(x,0) = f(x) \quad \text{in} \quad \Omega \tag{8}$$

$$B\left[u(x,t_n)\right] = g(x,t_n) \ ,\text{on} \quad \partial\Omega \, , \quad n = 1,\ldots,\mathrm{N}_t \tag{9}$$

where N_t is the number of time steps. So at each time step we have to solve a steady state problem by using finite collocation method.

2.1. Finite collocation method

In this method a set of points are selected in the domain and its boundary, randomly or regularly in which the total number of interior points of the domain is N. Around of each strictly-interior point, a stencil is considered, this interior point is called centerpoint of respective stencil. Connection of centerpoint to its surrounding points can be chosen in various forms like circle, square and other proper fashions. In this work, square stencils are chosen in size of 3× 3 and 5×5. Points in the stencils are divided as follows:

$$I_1 = \{x_1^b, x_2^b, \ldots, x_{m_1}^b\}, \qquad I_2 = \{x_1^i, x_2^i, \ldots, x_{m_2}^i\}, \tag{10}$$

s.t $\quad n(I_1) = k^2 - (k-2)^2 = m_1, \qquad n(I_2) = (k-2)^2 = m_2,$

where k is size of the stencil, I_1 is set of points that are placed on the stencil margin (solution centers) and I_2 is set of points in the interior of stencil (PDE centers) (see figure 1). Therefore in the domain of Ω in the relation (1), there are several overlapping stencils. Each stencil collocates L operator in its interior points (I_1) and collocates solution value in the marginal points of stencil. For each stencil, a local RBF collocation is proposed:

$$u(x) = \sum_{i=1}^{N} \alpha_i \phi_c(\|x - x_i\|_2), \tag{11}$$

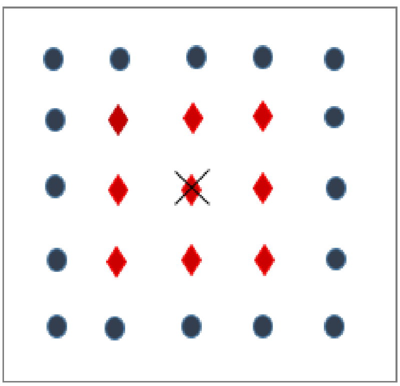

Figure 1: A stencil in size 5×5, Blue circles represent solution centers, Red diamonds show PDE centers and black cross show centerpoint.

where $\{x_1, x_2, \ldots, x_N\} \subset R^d$ is a set of points, $\|.\|$ is Euclidean norm and $\varphi(r)$ is a radial basis function. Parameter c is called shape parameter which play important role on function shape and must be chosen properly according to the situation.

and so that N local collocation systems can be obtain as follows:

$$A^{(s)}\lambda^{(s)} = d^{(s)} \qquad s = 1, 2, ..., N, \tag{12}$$

$$A^{(s)} = \begin{bmatrix} \left[A_b^{(s)}\right]^T \\ .... \\ \left[A_i^{(s)}\right]^T \end{bmatrix}, \tag{13}$$

where

$$\left[A_b^{(s)}\right] == \begin{bmatrix} \phi_c\left(\left\|x_1^b - x_1^b\right\|_2\right) & ... & \phi_c\left(\left\|x_{m_1}^b - x_1^b\right\|_2\right) \\ \phi_c\left(\left\|x_1^b - x_2^b\right\|_2\right) & ... & \phi_c\left(\left\|x_{m_1}^b - x_2^b\right\|_2\right) \\ \vdots & \cdots & \vdots \\ \phi_c\left(\left\|x_1^b - x_{m_1}^b\right\|_2\right) & \cdots & \phi_c\left(\left\|x_{m_1}^b - x_{m_1}^b\right\|_2\right) \\ \phi_c\left(\left\|x_1^b - x_1^i\right\|_2\right) & \cdots & \phi_c\left(\left\|x_{m_1}^b - x_1^i\right\|_2\right) \\ \vdots & \cdots & \vdots \\ \phi_c\left(\left\|x_1^b - x_{m_2}^i\right\|_2\right) & \cdots & \phi_c\left(\left\|x_{m_1}^b - x_{m_2}^i\right\|_2\right) \end{bmatrix}, \tag{14}$$

$$\left[A_i^{(s)}\right] == \begin{bmatrix} L\phi_c\left(\left\|x_1^i - x_1^b\right\|_2\right) & ... & L\phi_c\left(\left\|x_{m_2}^i - x_1^b\right\|_2\right) \\ L\phi_c\left(\left\|x_1^i - x_2^b\right\|_2\right) & ... & L\phi_c\left(\left\|x_{m_2}^i - x_2^b\right\|_2\right) \\ \vdots & \cdots & \vdots \\ L\phi_c\left(\left\|x_1^i - x_{m_1}^b\right\|_2\right) & \cdots & L\phi_c\left(\left\|x_{m_2}^i - x_{m_1}^b\right\|_2\right) \\ L\phi_c\left(\left\|x_1^i - x_1^i\right\|_2\right) & \cdots & L\phi_c\left(\left\|x_{m_2}^i - x_1^i\right\|_2\right) \\ \vdots & \cdots & \vdots \\ L\phi_c\left(\left\|x_1^i - x_{m_2}^i\right\|_2\right) & \cdots & L\phi_c\left(\left\|x_{m_2}^i - x_{m_2}^i\right\|_2\right) \end{bmatrix}, \tag{15}$$

and

$$\lambda^{(s)} = \begin{bmatrix} \alpha_1 \\ \alpha_2 \\ \vdots \\ \alpha_{m_1+m_2} \end{bmatrix} \qquad d^{(s)} = \begin{bmatrix} u_1 \\ u_2 \\ \vdots \\ u_{m_1} \\ f_{m_1+1} \\ \vdots \\ f_{m_1+m_2} \end{bmatrix}, \quad s = 1, 2, \ldots, N \tag{16}$$

where $\lambda^{(s)}$ is called interpolation coefficient and $d^{(s)}$ is data vectors of corresponding system. The vector $d^{(s)}$ includes values of (f_i) and (u_i) that (f_i) are values of L operator and (u_i) are unknown values in margin of stencil except that points are placed on the boundary of problem $(\partial\Omega)$. By using relation (11) we obtain:

$$u^{(s)}(x) = Q^{(s)}(x)\lambda^{(s)}, \tag{17}$$

which $Q^{(s)}$ is called a reconstruction vector for stencil s,

$$Q^{(s)}(x) = \left[\phi_c\left(\left\|x - x_1^b\right\|\right)\ldots\phi_c\left(\left\|x - x_{m_1}^b\right\|\right)\phi_c\left(\left\|x - x_1^i\right\|\right)\ldots\phi_c\left(\left\|x - x_{m_2}^i\right\|\right)\right].$$

After replacement of centerpoint, $x_c^{(s)}$, in (17) , we have:

$$\begin{aligned} u^{(s)}\left(x_c^{(s)}\right) &= Q^{(s)}\left(x_c^{(s)}\right)\lambda^{(s)} \\ &= Q^{(s)}\left(x_c^{(s)}\right)\left[A^{(s)}\right]^{-1} d^{(s)} \\ &= W^{(s)}\left(x_c^{(s)}\right)d^{(s)}, \end{aligned} \tag{18}$$

where vector $W^{(s)}\left(x_c^{(s)}\right) = Q^{(s)}\left(x_c^{(s)}\right)\left[A^{(s)}\right]^{-1}$ is called weight vector. Above equation is proposed for each stencil in centerpoints, so known values are placed on the right side of above equation and unknown values on the left side, so N simultaneous equations is obtained that led to a sparse global system. The approximation solution (u_i) is achieved by solving of this global system. It should be noted that when 5× 5 stencil or larger, intercept domain boundary, the usual method is to eliminate external points of domain that decrease the size of stencil (see figure.2(a)), but in order to maintaining of convergence rate, it is better that the size of stencils be considered fixed, thus stencil is shifted to the interior of the domain (see figure. 2(b))(26).

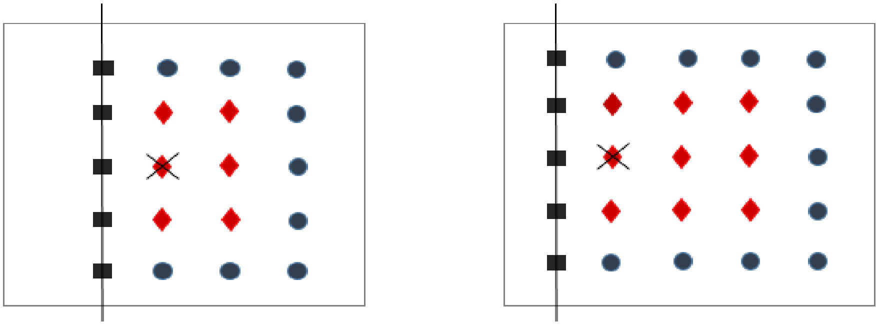

Figure 2: left figure show stencil truncation and right figure show stencil extension, square points are boundary values, Blue circles represent solution centers, Red diamonds show PDE centers and black cross show centerpoint.

2.2. Computational remarks

According to relation (13), the matrix $A^{(s)}, 1 \le s \le N$, only depends on distance of the points $\left(\left\| x_i - x_j \right\|, 1 \le i, j \le N\right)$, so it is enough that this matrix be computed just at a point. On the otherhand, vector $Q^{(s)}$ in 5×5 stencil should be computed in the nine cases. The first case is for places that stencil doesn't interrupt boundary of the domain, so it has not been shifted to interior of the domain (see figure 3). The next four cases are when stencil interrupt only one of the four boundaries of the domain. The last four cases are for the four points in corner of the domain that intercept two boundaries simultaneously. The above discussion and relation $W^{(s)}\left(x_c^{(s)}\right) = Q^{(s)}\left(x_c^{(s)}\right)\left[A^{(s)}\right]^{-1}$ show that we need to compute $W^{(s)}, 1 \le s \le N$, that isn't depends on s in case 3×3 stencil and so the value of $W^{(s)}$ in 5×5 stencil must be calculated only in nine points.

For computing $\varphi(x)$ at each time step, at first we solve global system and then reconstruction vector is used for collocation points as follow (25):

$$\hat{L}\left[u^n(x)\right] = \hat{L}\left[Q^{(s)}\left(x_c^{(s)}\right)\right]\left[A^{(s),n}\right]^{-1} d^{(s),n} = W_{\hat{L}}^{(s)}(x)\, d^{(s)}, 1 \le s \le N. \tag{19}$$

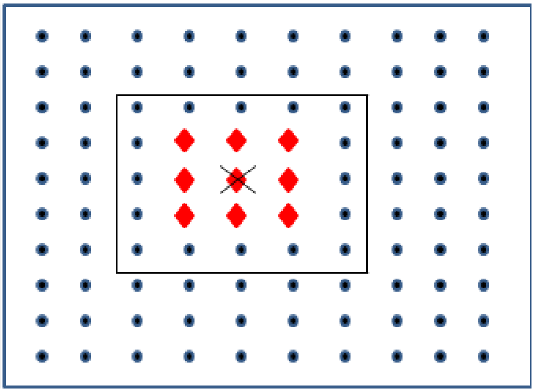

Figure 3: A stencil in size 5×5 in interior of domain

3. Numerical results

In this section, the local collocation method is described in section (2) based on multiquadric and inverse multiquadric basis $\left(\phi_c(r)=\sqrt{c^2+r^2}, \phi_c(r)=1/\sqrt{c^2+r^2}\right)$ is implemented for solving 2D unsteady convection-diffusion equation:

$$\frac{\partial u}{\partial t}=k_x\frac{\partial^2 u}{\partial x^2}+k_y\frac{\partial^2 u}{\partial y^2}+v_x\frac{\partial u}{\partial x}+v_y\frac{\partial u}{\partial y}, \tag{20}$$

such that $x_1, x_2\in[0,1]$ with the following Boundary and initial conditions:

$$u(0,y,t)=ae^{bt}\left(1+e^{-c_y y}\right), u(1,y,t)=ae^{bt}\left(e^{-c_x}+e^{-c_y y}\right)\quad t>0,$$

$$u(\mathrm{x},0,t)=ae^{bt}\left(1+e^{-c_x x}\right), u(\mathrm{x},1,t)=ae^{bt}\left(e^{-c_x x}+e^{-c_y}\right),$$

$$u(x,y,0)=a\left(e^{-c_x x}+e^{-c_y y}\right).$$

The exact solution is given by:

$$u(x,y,\mathrm{t})=ae^{bt}\left(e^{-c_x x}+e^{-c_y y}\right),$$

where $c_x=\dfrac{v_x\pm\sqrt{v_x{}^2+4k_x b}}{2k_x}>0, c_y=\dfrac{v_y\pm\sqrt{v_y{}^2+4k_y b}}{2k_y}>0$.

In this case $v_x = v_y = v$ and $k_x = k_y = k$ with Peclet number $pe = \frac{v}{k}$. Points is discretized with $M+1$ points in x,y directions $\left(N = M^2\right)$ and $N_t = \frac{T}{\Delta t}$ in t direction, here $\Delta t = 1/100$ and $T = 0.1$. Error is approximated by:

$$RE.error = \sqrt{\frac{\sum_{j=1}^{N^2}\left(u_j - \tilde{u}_j\right)^2}{N^2}},$$

where $\tilde{u}$ is approximation solution and u is exact solution. This problem has been solved with optimal values of shape parameters c_{opt} =3,2.9,2.8,2.5,2.9 for multiquadric basis and c_{opt} =1,2,4,4,5 for inverse basis and 3×3 stencil (see figure 4) .

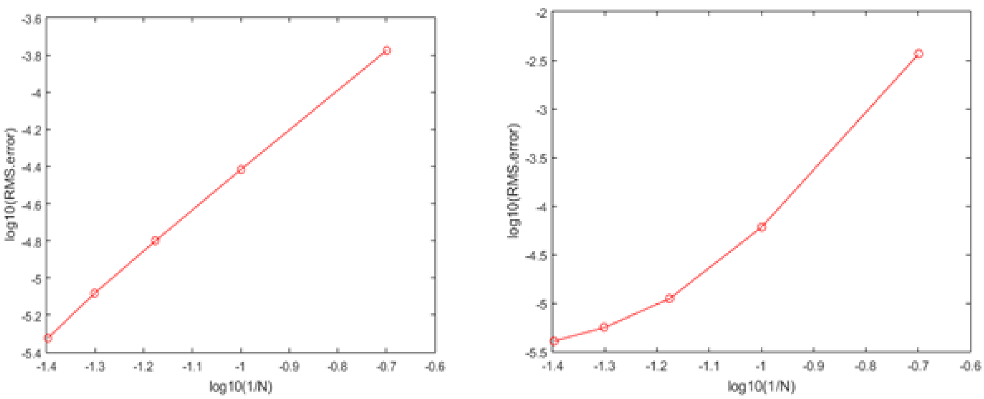

Figure 4: Relative error for 3× 3 stencil, left figure shows multiquadric method and right figure shows inverse method , θ =0.5 ,a=1 ,b=0.1 , Δ =1/100, v=1 , k=1 , pe=1.

The errors in the solution for different values of M=5,10,15,20,25 have been tabulated in table1 . These results show that errors in the solution decrease with increasing of points.

Table1: Relative error for 3×3 stencil and optimal shape parameter

N	c_{opt}	$RE.error\left(multiquadric\right)$	c_{opt}	$RE.error\left(inverse\right)$
25	3	1.6828274×10^{-4}	1	0.00365570
100	2.9	3.827216×10^{-5}	2	5.999228×10^{-5}
225	2.8	1.580940×10^{-5}	4	1.1091640×10^{-5}
400	2.5	8.280715×10^{-6}	4	5.5726202×10^{-6}
625	2.9	4.730291×10^{-6}	5	4.049818×10^{-6}

In case 5×5 stencil, results are obtained with optimal values of shape parameter c_{opt} =6.2,3.7,1.6,0.86,0.675 for multiquadric basis and c_{opt} =8.5,6,2,10.5,9 for inverse multiquadric basis, the errors of presented method for M=5,10,15,20,25 have been tabulated in table2 . These results verify validity and accuracy of presented method (see figure 5).

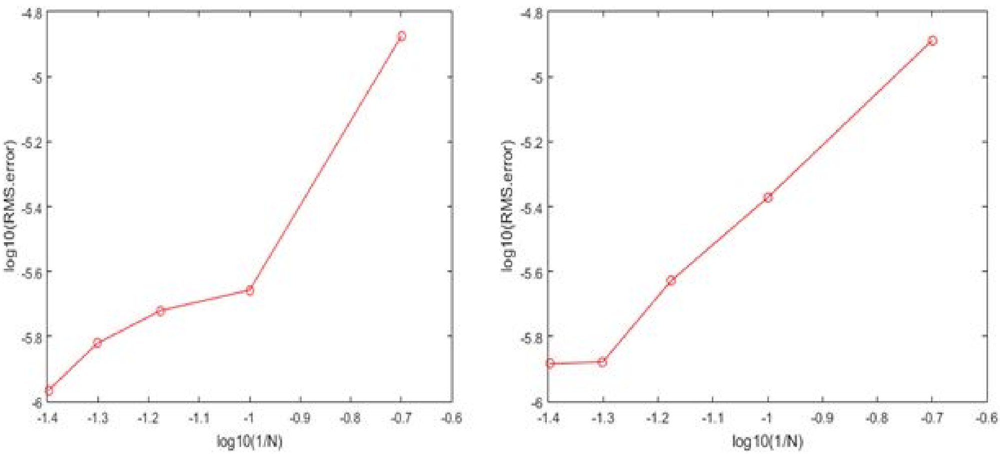

Figure 5:Relative error for 5×5 stencil, left figure shows multiquadric basis and right figure shows inverse basis, θ =0.5 , a=1 , b=0.1 , Δ =1/100, v=1, k=1 , pe=1.

Table2: Relative error for 5×5 stencil and optimal shape parameter

N	c_{opt}	$RE.error(multiquadric)$	c_{opt}	$RE.error(inverse)$
25	6.2	1.337038×10^{-5}	8.5	1.295745×10^{-5}
100	3.7	2.201251×10^{-6}	6	4.241687×10^{-6}
225	1.6	1.904626×10^{-6}	2	2.352594×10^{-6}
400	0.86	1.511389×10^{-6}	10.5	1.321409×10^{-6}
625	0.675	1.082512×10^{-6}	9	1.305637×10^{-6}

3. Conclusion

It is known that the global collocation method yield system that is ill-condition, but in the case of local collocation method, such ill-conditioning can be controlled. In this paper, the local collocation method based on multiquadric and inverse multiquadric basis is applied with two different stencils. The arising global system can be solved easily and the condition number of this system is low. The errors in tables 1and 2 show validity and accuracy of this approach. In addition for improving this algorithm and for reducing CPU time we explain this algorithm in matrix form. computational remarks in subsection (2.2) play key role in reducing computatioal time.

REFERENCES

1. Ascher Uri M., Ruuth Steven J. Wetton Brian T.R. Implicit-explicit methods for time-dependent partial differential equations, SIAM J. Numer. Anal., 32, 1995, pp.797-823.
2. Atluri S.N. The Meshless Method (MLPG) for Domain $\&$ BIE Discretizations,Tech Science Press, 2004.
3. Bayona V., Moscoso M., Carretero M., Kindelan M. RBF-FD formulas and convergence properties, J. Comput. Phys., 229, 2010, pp.8281-8295.
4. Bayona V., Moscoso M., Kindelan M. Optimal variable shape parameter for multiquadric based RBF-FD method, J. Comput. Phys., 231, 2012, pp.2466-2481.
5. Chen Y., Lee J., Eskandarian A. Meshless Methods in Solid Mechanics, Springer, 2006.
6. Dehghan M., Abbaszadeh M. A local meshless method for solving multi-dimensional Vlasov–Poisson and Vlasov–Poisson–Fokker–Planck systems arising in plasma physics, Engg. with Computer, 33, 2017, pp.961–981.
7. Dehghan M., Mohammadi V. A numerical scheme based on radial basis function finite difference (RBF-FD) technique for solving the high-dimensional nonlinear Schrödinger equations using an explicit time discretization: Runge–Kutta method, J.Comput. Phys. commun., 217, 2017, pp.23-34.
8. Duan Y. Meshless Galerkin method using radial basis functions based on domain decomposition, Appl. Math. Comput., 179, 2006, pp.750-762.
9. Flyer N., Lehto E., Blaise S., Wright G.B., St-Cyr A. A guide to RBF-generated finite differences for nonlinear transport: Shallow water simulations on a sphere, J. Comput. Phys., 231, 2012, pp.4078-4095.
10. Gao W., Wu Z. Solving time-dependent differential equations by multiquadric trigonometric quasi-interpolation, App.Math. Comput., 253, 2015, pp.377-386.
11. Griebel M., Schweitzer M. Meshfree Methods for Partial Differential Equations, Springer, 2002.
12. Griebel M., Schweitzer M. Meshfree Methods for Partial Differential Equations II, Springer, 2005.

13. Hajiketabi M., Abbasbandy S. The combination of meshless method based on radial basis functions with a geometric numerical integration method for solving partial differential equations: Application to the heat equation, Engg. Anal. with Bound. Element, 87, 2018, pp.36-46.
14. Johnson C., Nävert U., Pitkäranta, J. Finite element methods for linear hyperbolic problems, Comput. Appl. mech. eng. , 45, 1984, pp.285-312.
15. Kansa E.J. Multiquadrics – a scattered data approximation scheme with applications to computational fluid dynamics I: Surface approximations and partial derivatives estimates, Comput. Math. Appl., 19, 1990, pp.127-145.
16. Kansa E.J. Multiquadrics – a scattered data approximation scheme with applications to computational fluid dynamics II: Solution to parabolic, hyperbolic and elliptic partial differential equations, Comput. Math. Appl., 19, 1990, pp.147-161.
17. Leito V., Alves C., Durate C. Advances in Meshfree Techniques, Springer, 2007.
18. LeVeque R.J. Finite volume methods for hyperbolic problems, Publisher Cambridge university press, V.31,2002.
19. Liu G.R., Gu Y.T. An Introduction to Meshfree Methods and Their Programming, Springer, 2005.
20. Martin B., Fornberg B. Using radial basis function-generated finite differences (RBF-FD) to solve heat transfer equilibrium problems in domains with interfaces, Engg. Anal. with Bound. Elements,79, 2017, pp.38-48.
21. Meerschaert M.M., Tadjeran C. Finite difference approximations for two-sided space-fractional partial differential equations, Appl. numerical math., 56, 2006, pp.80-90.
22. Peaceman D.W., Rachford J.H.H. The Numerical Solution of Parabolic and Elliptic Differential Equations, J. Soc. Indust. Appl. Math., 3, 1955, pp.28-41.
23. Sarler B., Vertnik R. Meshless explicit local radial basis function collocation methods for diffusion problems, Comput. Math. Appl., 51, 2006, pp.1269 -1282.
24. Smith G.D. Numerical Solutions of Partial Differential Equations. Publisher Oxford university press,1985.
25. Stevens D., Power H., Lees M., Morvan H. The use of PDE centres in the local RBF Hermitian method for 3D convective-diffusion problems, J. Comput. Phys., 228, 2009, pp.4606-4624.
26. Stevens D., Power H., Meng C.Y., Howard D., Cliffe K.A. An alternative local collocation strategy for high –convergence meshless PDE solutions, using radial basis function, J. Comput. Phys., 254, 2013 pp.52-75.

27. Wendland H. Piecewise polynomial, positive definite and compactly supported radial basis functions of minimal degree, Adv. Comput. Math., 4, 1995, pp.389-396.
28. Wright G., Fornberg B. Scattered node compact finite difference-type formulas generated from radial basis functions, J. Comput. Phys., 212, 2006, pp.99-123.
29. Wu Z. Compactly supported positive definite radial basis functions, Adv. Comput. Math., 4, 1995, pp.75-97.
30. Zhou X., Hon Y. C., Li J. Overlapping domain decomposition method by radial basis functions, Appl. Numer, Math., 44, 2003, pp.241-255.
31. Zinober A.S.I., Huntley E. The numerical solution of linear time-dependent partial differential equations by the Laplace transform and finite difference approximations, Comput. Appl. Math., 6, 1980, pp.253-258.

Метод локального коллокации для решения уравнения конвекции-диффузии зависящего от времени

Джалил Рашидиния[1], Махди Махдави[1], Амирхосейн Собхани[1]
[1]Школа математики, Иранский университет науки и техники, Нармак, Хенгам, Тегеран, Иран
e-mail: rashidinia@iust.ac.ir

РЕЗЮМЕ

Для решения уравнения конвекции-диффузии зависящего от времени был представлен локальный метод коллокации RBF на основе мультиквадрического и обратного мультиквадрического базиса. Наша цель - сократить вычислительные затраты, предоставив матричную форму метода локального коллокации. Подход основан на квадратных трафаретах с размерами 3×3 и 5×5 вокруг каждой внутренней коллокации. Этот подход был применен для решения двумерного уравнения конвекции-диффузии путем преобразования задачи в разреженную глобальную систему линейных уравнений с малым числом условий. Полученные численные результаты подтверждают эффективный и точный характер нашего метода.

Ключевые слова: Многоквадратичная и обратная мультиквадрическая радиальная базисная функция, уравнение конвекции-диффузии зависящее от времени, метод конечной коллокации.